19th Brazilian Congress of Thermal Sciences and Engineering
November 6th–10th, 2022, Bento Gonçalves - RS - Brazil

ENC-2022-0519
ON THE USE OF CFD TO INVESTIGATE THE AEROELASTIC BEHAVIOR OF AN AIRFOIL

Bianca Taís Visoná Carnielo
Aluisio Viais Pantaleão
Douglas D. Bueno
São Paulo State University (UNESP) - Av. Brasil, 56 - Centro - Ilha Solteira/SP
bianca.carnielo@unesp.br, aluisio.pantaleao@unesp.br, douglas.bueno@unesp.br

Abstract. *Aeroelasticity is the branch which comprises studies involving interactions between structural and aerodynamic forces, mainly focusing on aerial vehicles. The fluid-structure interactions (FSI) can result in different phenomena to the system's dynamics, such as flutter, responses to buffeting loads, limit cycle oscillations, and others. Their solution usually requires both fluid and structure modeling. In this sense, the present work comprises aeroelastic simulations considering an airfoil NACA 0012 with two degrees of freedom. Different subsonic flow conditions are considered to investigate the airfoil with pitch and plunge motions. The fluid mesh is obtained by considering 133000 nodes, with refinement close to the airfoil shape to accurately represent the turbulent boundary layer. The structural mesh is developed by using the Finite Element Method. The meshes are connected by considering a strategy of interpolation. The solution uses the open source software SU2 supported by the SU2 Foundation, which allows one to couple the computational code with an algorithm written in Python. The results show the system responses for both degrees of freedom for different Mach numbers, in both time and frequency domains. The general behavior is asymptotically stable due to the aerodynamic damping because the structural damping is neglected. The results demonstrate that the employed methodology is suitable for solving this type of fluid structure interaction problem and the approach offers promise for further investigations involving fluid and structure nonlinearities.*

Keywords: *fluid structure interaction, aeroelasticity, SU2, computational fluid dynamics*

1. INTRODUCTION

Aeroelasticity is a science which studies the mutual interaction between aerodynamic forces and elastic forces, and the influence of this interaction on airplane design. Modern airplane structures are very flexible, and this flexibility is fundamentally responsible for the various types of aeroelastic problems (Bisplinghoff *et al.*, 1996).

This interaction of a flexible structure with a flowing fluid in which it is submersed gives rise to a variety of physical phenomena such as flutter, responses to buffeting loads, limit cycle oscillations, and others. To understand these phenomena it is necessary to model both the structure and the fluid (Dowell and Hall, 2001). Once it must be light, an airplane deforms due to the load, these deformations change the distribution of the aerodynamic forces, which in turn changes the deformations. This process may lead to flutter, a self-excited oscillation. Since flutter involves the problems of interaction of aerodynamics and structural deformation, it involves aspects of fluid-structure analysis (Garrick and Reed, 1981).

Fluid structure interaction (FSI) techniques have been widely used in many industrial problems for aerospace applications. It is performed aeroelastic computations by means of a coupled approach with these techniques where the aerodynamic forces are computed from the solution of the Navier-Stokes equations (Guerri *et al.*, 2008). The solution of Navier-Stokes equations is developed by Computational Fluid Dynamics (CFD), that is a branch of fluid mechanics that uses numerical methods and computational algorithms to solve complex problems involving fluid flow (Dash, 2016).

In particular, solutions to FSI problems in aeronautics can be obtained using the free software SU2, created by the *SU2 Foundation*, and developed and maintained by Stanford University, USA (SU2 Foundation, 2022). The software has been used to solve several problems, including in the transonic regime, as shown by Economon *et al.* (2016) and Ryabinin and Kuzmin (2020). The FSI coupling approach employed in SU2 is described by Sanchez *et al.* (2016). The authors evaluate the software's ability to perform aeroelastic analysis using computational tools, and also employing communication with external computational code through a wrapper resource written in Python.

In the analysis of complex structures, there is a finite element model for a structural body undergoing oscillations that

reduces in size by first finding the natural or eigenmodes of the structure and then recasting the finite element structural model in terms of these modes. Usually, a finite element structural model of a few thousand degrees of freedom is reduced to a modal model with a few tens of degrees of freedom. This reduces not only the size of the model but also the computational cost by orders of magnitude (Dowell and Hall, 2001).

Fonzi *et al.* (2021) developed an update of the Python–based fluid structure interaction framework of SU2 code and extended it to allow efficient and fully open source simulations of aeroelastic phenomena. It was also introduced a native code to solve the structural equations coming from a Nastran–like Finite Element Model. In this sense, the present work comprises aeroelastic simulations applying the SU2 fluid structure interaction methodology. The airfoil NACA 0012 with two degrees of freedom is considered. Different subsonic flow conditions are evaluated to investigate the airfoil with pitch and plunge motions in the subsonic flow, which correspond to the Mach numbers equal to 0.20, 0.23, 0.25, 0.27, 0.34 and 0.36, in both time and frequency domains.

2. METHODOLOGY

The aeroelastic system investigated in this article is the NACA 0012 airfoil with two degrees of freedom (DOF). They correspond to the pitch angle (α) and the plunge (h) DOFs, and the system is illustrated in Fig. 1. The numerical solution is obtained by employing the open source software SU2, which is supported by the SU2 Foundation. It allows one to couple the computational code developed to solve the fluid dynamics with an algorithm written in Python to solve the structural dynamics.

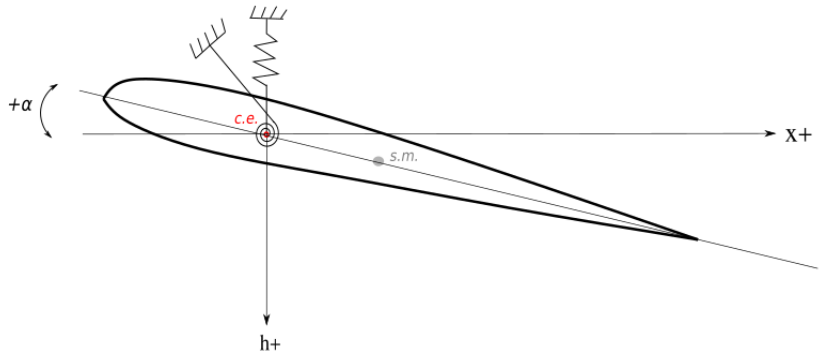

Figure 1. Airfoil with two degrees of freedom, where h is plunge and α is pitch degrees of freedom.

The structural model is obtained by considering a single point placed at the rotation axis (i.e., the elastic center). It is the master node, and the airfoil inertia and mass properties are both considered concentrated at the center of mass of the profile. The Finite Element Method is employed to obtain the structural mesh, and it is obtained from the software Nastran. The mass and stiffness matrices are both written in the generalized coordinate system, and the modal shapes are normalized in terms of mass. The structural mesh consists in a set of rigid elements which connect 123 nodes to the master node. Each node has two degrees of freedom, such as the airfoil. Figure 2 shows an illustrative scheme of the structural mesh. Note that the structural mesh does not correspond to the airfoil shape, and this strategy is employed to write the aerodynamic forces on this mesh more accurately (Fonzi *et al.*, 2021).

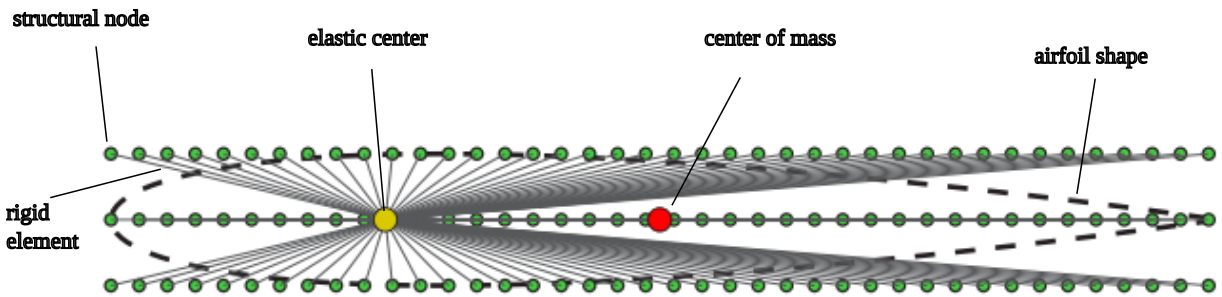

Figure 2. Airfoil shape and structural mesh.

The generalized coordinate system is achieved by using the modal matrix ($\mathbf{\Phi}$) obtained by extracting the eigenvectors from the associated structural undamped vibration problem. The physical displacement vector $\mathbf{u}$ is defined by including the vertical direction (perpendicular to the x-axis shown in Fig. 1) and the rotation angle similar to the pitch DOF, i.e,

respectively y_i and $\theta_{z(i)}$, such that

$$\mathbf{u} = \{y_1 \;\; \theta_{z1} \;\; y_2 \;\; \theta_{z2} \;\; y_3 \;\; \theta_{z3} \;\; \ldots \;\; y_{123} \;\; \theta_{z123}\}^T \tag{1}$$

Rigid elements are connected to the master node, and because of this strategy only two eigenvectors are considered to describe the vibrating modes of interest, i.e., $\mathbf{\Phi} = [\mathbf{\Phi}_y \;\; \mathbf{\Phi}_\theta]$. The physical displacement vector is rewritten in terms of the generalized coordinates $\mathbf{u}_\Phi$ by the following equation

$$\mathbf{u} \cong [\mathbf{\Phi}_y \;\; \mathbf{\Phi}_\theta]\mathbf{u}_\Phi \tag{2}$$

where $\mathbf{\Phi}_y$ and $\mathbf{\Phi}_\theta$ are the undamped structural modes respectively related to plunge and pitch DOFs.

The FSI solution begins with the fluid code obtaining the aerodynamic forces for the initial condition. The aerodynamic model is based on the Reynolds Averaged Navier-Stokes (RANS) equations, with Menter's Shear Stress Transport (SST) turbulence model. According to Versteed and Malalasekera (2007), the equations for describing the continuity (Eq. 3) and Navier-Stokes equations (Eq. 4) are respectively given by

$$\frac{\partial \bar{\rho}}{\partial t} + \mathrm{div}(\bar{\rho}\tilde{\mathbf{U}}) = 0 \tag{3}$$

where ρ is the air specific mass, $\mathrm{div}\,(\;)$ is the divergent operator, and $\mathbf{U} = \{U \;\; V\}^T$ is the average velocities vector, respectively in the x and y directions. In addition,

$$\begin{aligned}
\frac{\partial(\bar{\rho}\tilde{U})}{\partial t} + \mathrm{div}(\bar{\rho}\tilde{U}\tilde{\mathbf{U}}) &= -\frac{\partial \bar{P}}{\partial x} + \mathrm{div}(\mu\,\mathrm{grad}\,\tilde{U}) + \left[-\frac{\partial\overline{(\bar{\rho}u'^2)}}{\partial x} - \frac{\partial\overline{(\bar{\rho}u'v')}}{\partial y}\right] + S_{Mx} \\
\frac{\partial(\bar{\rho}\tilde{V})}{\partial t} + \mathrm{div}(\bar{\rho}\tilde{V}\tilde{\mathbf{U}}) &= -\frac{\partial \bar{P}}{\partial y} + \mathrm{div}(\mu\,\mathrm{grad}\,\tilde{V}) + \left[-\frac{\partial\overline{(\bar{\rho}u'v')}}{\partial x} - \frac{\partial\overline{(\bar{\rho}v'^2)}}{\partial y}\right] + S_{My}
\end{aligned} \tag{4}$$

where u' and v' are the airspeed unsteady components in x e y directions, P is the aerodynamic pressure and S_M is the source term. The notation $\bar{(\;)}$ indicates average in time and $\tilde{(\;)}$ indicates that the parameter is weighted by the average density. The instantaneous velocities in x and y directions are $u = U + u'$ e $u = V + v'$, respectively. The fluid domain is discretized with 133000 nodes, and refined close to the airfoil surface to represent the turbulent boundary layer. The aerodynamic forces ($\tilde{F}_a$) are obtained by the CFD solution and it is interpolated from the fluid mesh to the structural mesh. The interpolation process is performed by the RBF (Radial Basis Functions) method. The radial basis interpolation depends on a given continuous function (φ) and a distance (radius) and additional details can be found in reference Buhmann (1990)). In this present article the kernel function (φ) is given by

$$\varphi = (1-r)^4(4r+1) \tag{5}$$

where r is the Euclidian distance between the fluid and solid points divided by the RBF radius of 0.5. After interpolating the aerodynamic forces, they are known in the structural nodes (i.e., it is $\mathbf{F}_a$). This aerodynamic force vector is considered to compute the corresponding structural displacements. The aeroelastic equation of motion is given by

$$\mathbf{M}\ddot{\mathbf{u}} + \mathbf{K}\mathbf{u} = \mathbf{F}_a \tag{6}$$

It is rewritten in the generalized coordinate system by $\mathbf{M}\mathbf{\Phi}\ddot{\mathbf{u}}_\Phi + \mathbf{K}\mathbf{\Phi}\mathbf{u}_\Phi = \mathbf{F}_a$, and pre-multiplying it by $\mathbf{\Phi}^T$, it is obtained $\mathbf{\Phi}^T\mathbf{M}\mathbf{\Phi}\ddot{\mathbf{u}}_\Phi + \mathbf{\Phi}^T\mathbf{K}\mathbf{\Phi}\mathbf{u}_\Phi = \mathbf{\Phi}^T\mathbf{F}_a$. The final equation of motion is given by the following equation

$$\mathbf{M}_\Phi\ddot{\mathbf{u}}_\Phi + \mathbf{K}_\Phi\mathbf{u}_\Phi = \mathbf{F}_{a\Phi} \tag{7}$$

The solution of this equation for the next time step (dt) allows one to compute new displacement vector, which is used to recompute the mesh of the fluid. Then, the procedure presented herein is repeated until achieving the n_t points such that the maximum time is equal to $t \equiv t_{max} = (n_t - 1)dt$.

3. RESULTS AND DISCUSSION

This section presents numerical results computed for the airfoil in different Mach numbers shown in Tab. 1. The fluid mesh for the first time step (i.e., $t = 0$) is illustrated in Fig. 3. The initial condition corresponds to the pitch angle of 5 degrees with the horizontal direction. The generalized mass and stiffness matrices are shown below. Note that they are diagonal matrices, and 199.9 and 2773.9 are both the first and second eigenvalues extracted from the associated undamped structural problem.

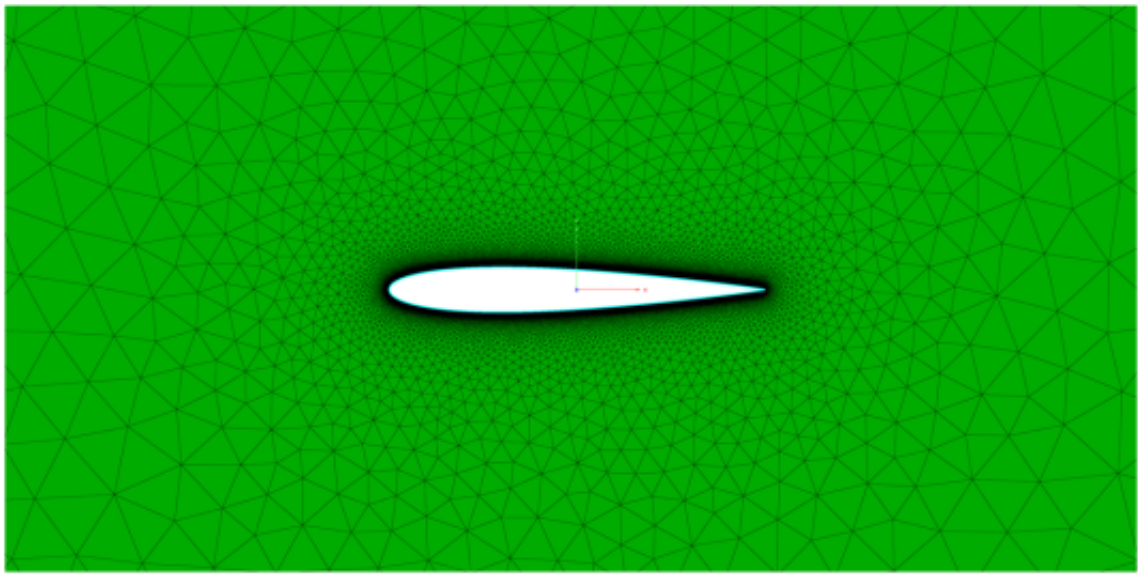

Figure 3. Aerodynamic mesh for the first time step.

$$\mathbf{M}_\Phi = \begin{bmatrix} 1 & 0 \\ 0 & 1 \end{bmatrix} \qquad \mathbf{K}_\Phi = \begin{bmatrix} 199.9 & 0 \\ 0 & 2773.9 \end{bmatrix}$$

Table 1 presents the corresponding plunge and pitch frequencies, which are shown in Fig. 4. These results demonstrate for the Mach number range considered that the energy of motion do not change the aeroelastic modal frequencies substantially. Numerical results are obtained those six different Mach number by performing time integration from zero to 4 seconds. The pitch responses for each Mach number are presented in Fig. 5. Similarly, Fig. 6 shows the plunge responses and both results indicate that the airfoil is stable, i.e., there is no flutter until Mach number equal to 0.36. The results also demonstrate that the aeroelastic damping is higher for the pitch degree of freedom once the α angle is almost zero before achieving 2 seconds of motion, whereas the plunge DOF continues oscillating until 4 seconds.

Table 1. Frequency values for each Mach number.

Mach Number	Plunge Freq.	Pitch Freq.
0.20	2.5352	7.6056
0.23	2.5352	7.6056
0.25	2.5352	7.6056
0.27	2.5352	7.6056
0.34	2.8169	7.0423
0.36	2.8169	7.0423

Figure 7 shows that the pitch responses contain more energy than the plunge. However, its energy decays with increasing Mach number, whereas the plunge energy increases. These results are presented by normalizing the values in respect to the maximum energy, which corresponds to the pitch DOF at Mach number 0.20. The results suggest that a possible flutter mechanism may occur by involving an increasing contribution from the plunge mode. However, further investigations need to be done to evaluate the airfoil in an unstable condition.

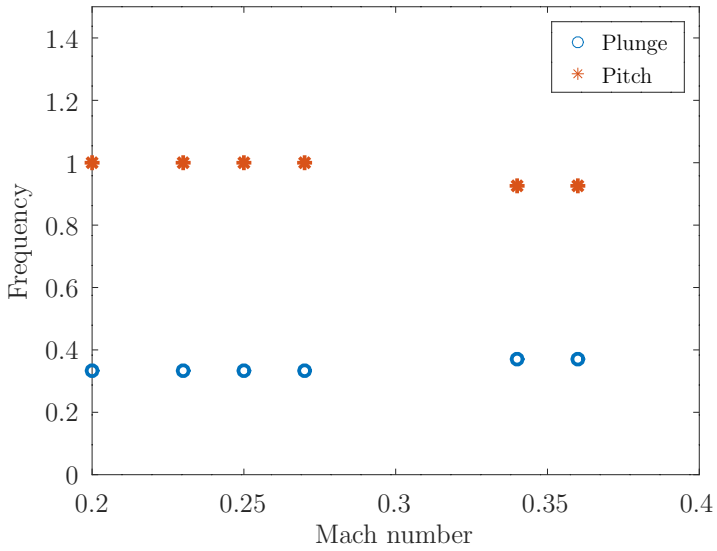

Figure 4. Pitch and plunge aeroelastic frequencies for each Mach number, normalized by the pitch frequency for $M_a = 0.20$ (i.e., 7.6056 Hz).

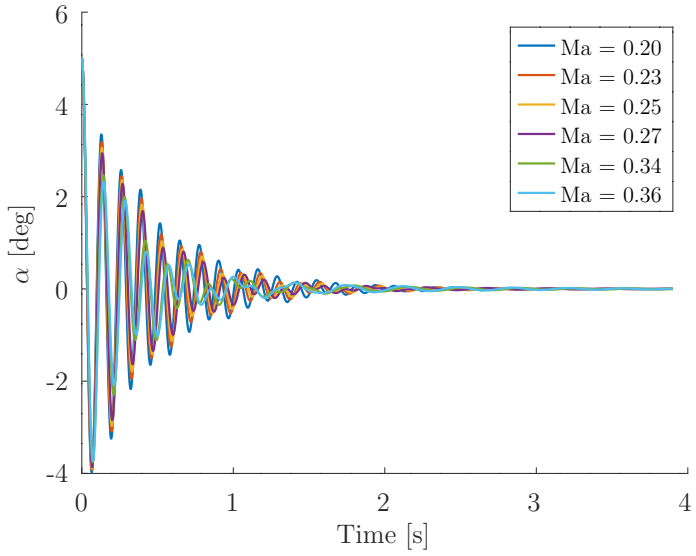

Figure 5. Pitch motion over time for each Mach number.

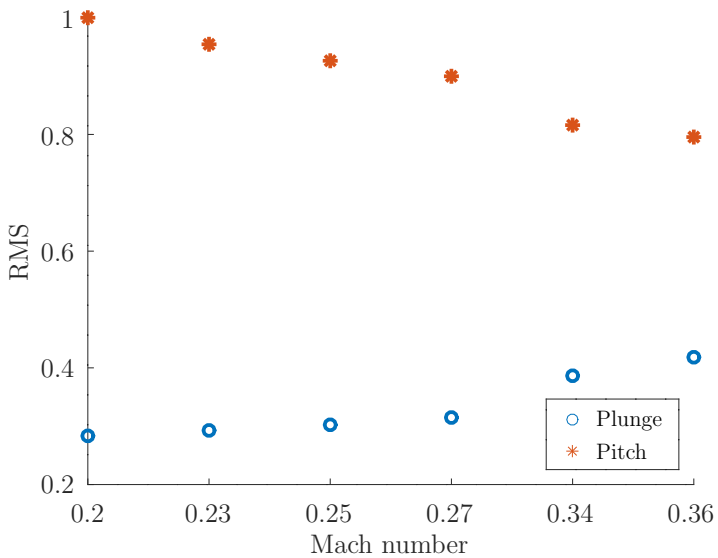

Figure 7. RMS values of pitch and plunge motion for each Mach number, normalized by $M_a = 0.20$ RMS pitch.

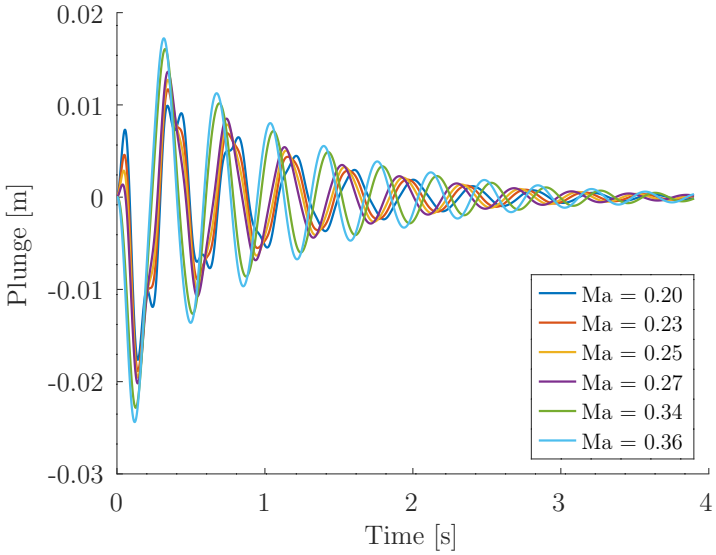

Figure 6. Plunge motion over time for each Mach number.

Table 2. RMS values for each Mach number.

Mach Number	RMS Plunge	RMS Pitch
0.20	$3.99 \times 10^{-}3$	$1.41 \times 10^{-}2$
0.23	$4.12 \times 10^{-}3$	$1.34 \times 10^{-}2$
0.25	$4.25 \times 10^{-}3$	$1.30 \times 10^{-}2$
0.27	$4.43 \times 10^{-}3$	$1.27 \times 10^{-}2$
0.34	$5.44 \times 10^{-}3$	$1.15 \times 10^{-}2$
0.36	$5.89 \times 10^{-}3$	$1.12 \times 10^{-}2$

The results in frequency domain are presented in Fig. 8 and Fig. 9. The changes in Mach numbers implies small variations in the aeroelastic frequencies, such as previously shown in Table 1. The results for the first four Mach number considered herein demonstrate the same frequencies for the aeroelastic system, and there is a small increasing for the plunge and decrease for the pitch DOFs.

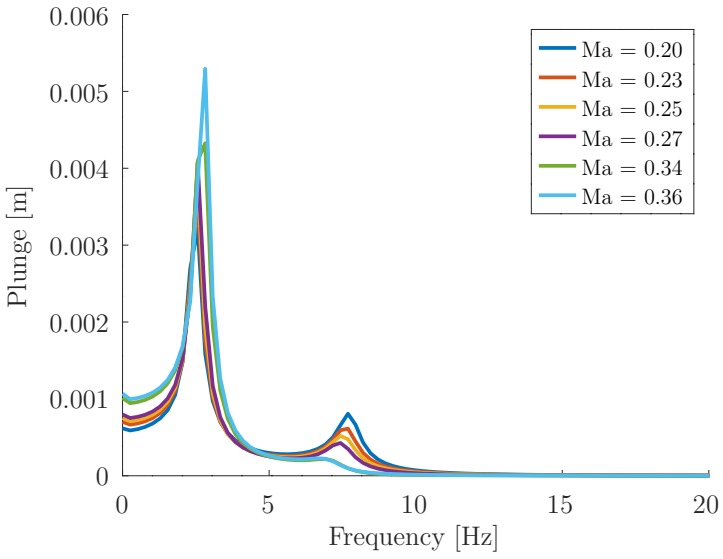

Figure 8. Frequency response functions for the plunge motion for each Mach number investigated in the present article.

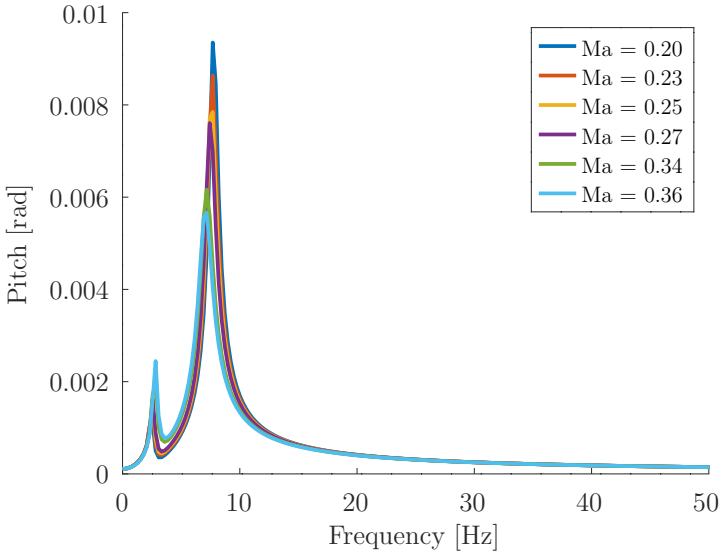

Figure 9. Frequency response functions for the pitch motion for each Mach number investigated in the present article.

4. CONCLUSIONS

The present article introduced a methodology to investigate the aeroelastic behavior of an NACA 0012 airfoil involving a fluid and structure interaction (FSI) based approach. The study includes the pitch and plunge degrees of freedom and it was carried out by using the free software SU2. The analysis of the responses over time showed that the pitch and plunge DOFs are stable for all Mach numbers investigated. This behavior means that there is no flutter until Mach number 0.36. It is possible to observe that the pitch aeroelastic damping is greater than the plunge one, since in this first DOF the oscillations end close to 2 seconds of motion, whereas for the second DOF the oscillations still happening until 4 seconds. However, when analyzing the RMS values of the degrees of freedom for each Mach number, it is noted that the pitch degree of freedom has more energy than the plunge DOF, and the pitch energy decays with the Mach number increasing, whereas the opposite behavior is verified to the plunge DOF.

The results in the frequency domain demonstrate that increase in Mach number implies small changes in the aeroelastic frequency, which means that the flutter point may be in a higher Mach number. The results also demonstrate that the employed methodology is suitable for solving this type of fluid structure interaction problem. Future efforts will be done to determine the Mach number in which the system becomes unstable, i.e., to find the flutter phenomenon.

5. ACKNOWLEDGEMENTS

The authors thank CNPq (National Council for Scientific and Technological Development) Grant numbers 152168/2021-4 (first author) and 314151/2021-4 (third author).

6. REFERENCES

Bisplinghoff, R.L., Ashley, H. and Halfman, R.L., 1996. *Aeroelasticity*. Dover Plublications, Inc.

Buhmann, M.D., 1990. "Multivariate interpolation in odd-dimensional euclidean spaces using multiquadrics". *Constructive Approximation*, Vol. 6, No. 1, pp. 21–34. doi:10.1007/bf01891407.

Dash, A., 2016. "CFD analysis ofWind turbine airfoil at various angles of attack". *IOSR Journal of Mechanical and Civil Engineering*, Vol. 13, No. 04, pp. 18–24. doi:10.9790/1684-1304021824.

Dowell, E.H. and Hall, K.C., 2001. "Modeling of fluid structure interaction". *Annual Review of Fluid Mechanics*, Vol. 33, No. 1, pp. 445–490. doi:10.1146/annurev.fluid.33.1.445.

Economon, T.D., Palacios, F., Copeland, S.R., Lukaczyk, T.W. and Alonso, J.J., 2016. "SU2: An open-source suite for multiphysics simulation and design". *AIAA Journal*, Vol. 54, No. 3, pp. 828–846. doi:10.2514/1.j053813.

Fonzi, N., Cavalieri, V., Gaspari, A.D. and Ricci, S., 2021. "Advances of the python–based fluid–structureinteraction capabilities included in su2". *arXiv preprint arXiv:2109.12332*.

Garrick, I.E. and Reed, W.H., 1981. "Historical development of aircraft flutter". *Journal of Aircraft*, Vol. 18, No. 11, pp. 897–912. doi:10.2514/3.57579.

Guerri, O., Hamdouni, A. and Sakout, A., 2008. "Fluid structure interaction of wind turbine airfoils". *Wind Engineering*, Vol. 32, No. 6, pp. 539–557. doi:10.1260/030952408787548875.

Ryabinin, A. and Kuzmin, A., 2020. "Transonic flow simulation in a bent channel using SU2 software". In *2020 Ivannikov Ispras Open Conference (ISPRAS)*. IEEE. doi:10.1109/ispras51486.2020.00034.

Sanchez, R., Kline, H.L., Thomas, D., Variyar, A., Righi, M., Economon, T., Alonso, J.J., Palacios, R., Dimitriadis, G. and Terrapon, V., 2016. "Assessment of the fluid-structure interaction capabilities for aeronautical applications of the open-source solver su2". *VII European Congress on Computational Methods in Applied Sciences and Engineering*.

SU2 Foundation, 2022. "SU2 official website". URL `https://su2code.github.io/`.

Versteed, H.K. and Malalasekera, W., 2007. *An introduction to computational fluid dynamics*. Pearson, 2nd edition.

7. RESPONSIBILITY NOTICE

The authors are solely responsible for the printed material included in this paper.